

Atypical Retardation Patterns in Scanning Laser Polarimetry Are Associated with Low Peripapillary Choroidal Thickness

Ralf P. Tornow,¹ Wolfgang A. Schrems,¹ Delia Bendschneider,¹ Folkert K. Horn,¹ Markus Mayer,^{2,3} Christian Y. Mardin,¹ and Robert Lämmer¹

PURPOSE. Scanning laser polarimetry (SLP) results can be affected by an atypical retardation pattern (ARP). One reason for an ARP is the birefringence of the sclera. The purpose of this study was to investigate the influence of the peripapillary choroidal thickness (pChTh) on the occurrence of ARP.

METHODS. One hundred ten healthy subjects were investigated with SLP and spectral domain OCT. pChTh was measured in B-scan images at 768 positions using semiautomatic software. Values were averaged to 32 sectors and the total peripapillary mean. Subjects were divided into four groups according to the typical scan score (TSS) provided by the GDxVCC: group 1 TSS, 100; group 2 TSS, 90–99; group 3 TSS, 80–89; group 4 TSS, <80.

RESULTS. Mean pChTh (\pm SD) in 110 healthy subjects was 141 μm ($\pm 49 \mu\text{m}$). There was a significant correlation between pChTh and TSS ($r = 0.608$; $P < 0.001$). In TSS groups 1 to 4, mean pChTh was 168 μm ($\pm 38 \mu\text{m}$), 148 μm ($\pm 48 \mu\text{m}$), 119 μm ($\pm 35 \mu\text{m}$), and 92 ($\pm 42 \mu\text{m}$). Mean pChTh of TSS groups 3 and 4 was significantly lower than that of TSS group 1 ($P < 0.001$).

CONCLUSIONS. Low values of TSS resulting from the appearance of ARP in SLP are associated with low peripapillary choroidal thickness. Reduced choroidal thickness may result in an increased amount of confounding light getting to the SLP light detectors. (*Invest Ophthalmol Vis Sci.* 2011;52:7523–7528) DOI:10.1167/iovs.11-7557

The thickness of the retinal nerve fiber layer (RNFL) is an important parameter in glaucoma research and in clinical practice. There are different methods to assess the RNFL thickness. The most widely used noninvasive imaging techniques to quantitatively evaluate peripapillary RNFL thickness are scanning laser polarimetry (SLP) and optical coherence tomogra-

phy (OCT). Both methods use different optical principles to assess RNFL thickness. OCT is based on low coherence interferometry.¹ RNFL thickness can be calculated from high-resolution cross-sectional images (B-scans) of the retinal layers by automatically segmenting the upper and lower borders of the RNFL.²

SLP uses the polarization properties of light to determine phase retardation induced by the birefringence of the RNFL. By conversion of RNFL-induced phase retardation using a fixed conversion factor, RNFL thickness is estimated.³ However, other parts of the eye, especially the cornea, also show birefringence and introduce phase retardation to the probing laser beam. The corneal birefringence can be compensated. The commercial instrument GDx (developed by Laser Diagnostic Technologies, now sold by Carl Zeiss Meditec, Jena, Germany) uses continuously improved techniques for compensating corneal birefringence. In the early commercial instrument, GDxFCC, a corneal compensator with fixed retardation (60 nm) and axis orientation (fast axis 15° nasally downward) was used to minimize the retardation introduced by the cornea. The next generation, GDxVCC, was equipped with variable corneal compensation (VCC) and uses the macular birefringence pattern to measure and neutralize for the corneal birefringence in each eye individually. SLP with variable corneal compensation provides a more accurate measurement of RNFL compared to SLP with fixed compensation.⁴ The latest version of the GDx uses an enhanced corneal compensation (ECC) technique to compensate corneal birefringence. In the ECC mode, the corneal compensator is adjusted so that it combines with corneal retardation to produce a bias retardation of approximately 55 nm into the signal path and with the slow axis close to vertical. In this way, the SLP measures a higher total retardation than the RNFL retardation alone, and the signal-to-noise ratio is improved. The actual RNFL retardation is derived mathematically.⁵ However, ECC results cannot be mathematically derived from the older existing VCC result; instead, ECC has to be available during data acquisition.

Both OCT and SLP have high diagnostic value for glaucoma detection (for example, see Refs. 6, 7). However, in a subset of normal and glaucomatous eyes, SLP results show an atypical retardation pattern (ARP).⁸ An ARP is a retardation pattern that cannot be explained by the distribution of the retinal nerve fibers. An ARP produces an artifactual increase in RNFL thickness.⁸ Bagga et al.⁸ developed a method to identify and quantify ARP based on a support vector machine (SVM). The developed SVM score ranges from 0 to 100. SLP retardation images with an SVM score of 100 have the most typical retardation pattern; lower scores are associated with greater image atypia. The SVM score is highly predictive of ARP images. In the commercial instrument, ARP is quantified by the typical scan score (TSS) with the same range.

From the ¹Universitätsklinikum Erlangen, Augenklinik, Erlangen, Germany; and ²Pattern Recognition Lab and ³Erlangen Graduate School in Advanced Optical Technologies, University Erlangen-Nuremberg, Erlangen, Germany.

Presented at the annual meeting of the Association for Research in Vision and Ophthalmology, Fort Lauderdale, Florida, May 2010.

Supported by German Research Foundation (Grant SFB 539), University of Erlangen-Nuremberg (ELAN-Fonds), and Erlangen Graduate School in Advanced Optical Technologies.

Submitted for publication March 15, 2011; revised July 14, 2011; accepted July 28, 2011.

Disclosure: **R.P. Tornow**, None; **W.A. Schrems**, None; **D. Bendschneider**, None; **F.K. Horn**, None; **M. Mayer**, None; **C.Y. Mardin**, None; **R. Lämmer**, None

Corresponding author: RalfPeter Tornow, Department of Ophthalmology, Universitätsklinikum Erlangen, Schwabachanlage 6, 91054 Erlangen, Germany; ralf.tornow@uk-erlangen.de.

Given that RNFL thickness measured from OCT B-scans is not affected by other layers, OCT RNFL thickness measurements in the same subjects can be used to verify SLP RNFL thickness results. It was shown with high spatial resolution that decreasing TSS results in increasing RNFL thickness error and an overestimation of the RNFL thickness, primarily in the temporal and nasal quadrants.⁹

The diagnostic performance of RNFL thickness parameters assessed with GDxVCC is significantly reduced because of ARP.¹⁰ Bowd¹¹ showed that the diagnostic accuracy of GDxVCC parameters is affected by disease severity and is adversely affected by the presence of atypical retardation patterns. They conclude that GDxVCC scans with atypical scan patterns should be interpreted with caution when used in clinical practice.

The ECC technique performed significantly better than VCC for diagnosing glaucoma in patients with ARP and earlier stages of the disease.¹²⁻¹⁴ However, despite the improved technique, uncompensated ARPs remain in some subjects (for example, see Ref. 15). Improved knowledge of the origin of ARP in GDxVCC is useful for basic research into the interaction of light with retinal layers and for clinical applications. It was shown that ARP and TSS can change over time and can have a significant effect on the detection of progressive RNFL loss with GDxVCC.¹⁶ Because statistically significant differences were found between GDxVCC and GDxECC results,¹⁷ GDxVCC is still to be used for reliable follow-up studies that started before GDxECC was commercially available.

The physical principles for the development of an ARP are not yet fully understood. Using an experimental polarization-sensitive OCT, it was shown that the physical origin of the confounding retardation is most likely the highly birefringent sclera.¹⁸ However, the reason some subjects show atypical patterns and others do not is still unclear. A parameter that has not been considered thus far but that can have an impact on the development of ARP is choroidal thickness. The purpose of this study was to measure the influence of peripapillary choroidal thickness in healthy subjects at the occurrence of ARP in SLP.

SUBJECTS AND METHODS

Subjects

One hundred ten healthy subjects were included in this study and were recruited through the Erlangen Glaucoma Registry (www.clinicaltrials.gov, NCT 00494923). All subjects underwent standard ophthalmic examination, including slit-lamp inspection, perimetry, funduscopy, gonioscopy, and papillometry. Optic disc evaluations were based on 15° color photographs (Telecentric fundus camera; Zeiss, Jena, Germany). Subjects were excluded if refractive error exceeded 5 diopters (D) equivalent sphere or 5 D astigmatism. Subjects had no systemic disease that could affect the eye. Findings in slit-lamp inspection were normal, and no pathologic changes were found on fundus examination. Optic discs were inspected and classified as normal by at least two experienced ophthalmologists. One randomly selected eye of each subject was used in this study. The study was approved by our institutional review board and complied with the tenets of Declaration of Helsinki. Informed consent was obtained from all participants in the study.

Perimetry

All subjects underwent visual field tests with standard white-on-white perimetry with a computerized static projection perimeter (Octopus 500; Haag-Streit, Bern, Switzerland). All subjects had normal visual field test results. Visual field loss was defined as a cluster of three or more adjacent points with $P < 0.05$ or two or more adjacent points with $P <$

0.01 on the pattern deviation map. The false-negative and false-positive rate had to be lower than 12%.

Scanning Laser Polarimetry

Scanning laser polarimetry (SLP) was performed using GDxVCC. The images provided by GDxVCC were analyzed with software version 5.5.0. To ensure accurate corneal measurement, the software provides an image quality check score (range, 1-10) based on the correct alignment, fixation, and refraction of the scan. Only scans with a centered optic disc, a sharp and evenly illuminated reflectance image, and a quality score of 9 or 10 (not to be confounded with TSS) were accepted in the present study. RNFL thickness measurements were obtained in an annulus around the optic disc (inner diameter, 2.51 mm; outer diameter, 3.26 mm). RNFL thickness values of 64 sectors and TSS were exported. All TSS values are included. Subjects were divided into four groups according to their TSS provided by the GDxVCC (Table 1): very typical (TSS 100), typical (TSS 90-99), less typical (TSS 80-89), and atypical (TSS <80).

Optical Coherence Tomography

All subjects underwent imaging with a commercially available spectral domain OCT system (SD-OCT; Spectralis HRA+OCT; Heidelberg Engineering, Heidelberg, Germany). Infrared reflection images ($\lambda = 820$ nm) and OCT B-scans ($\lambda = 870$ nm; A-scans 40,000/s) of the dual laser scanning systems were acquired simultaneously. Sixteen consecutive circular B-scans (3.4-mm diameter, 768 A-scans) centered at the optic disc were automatically averaged to reduce speckle noise. An online tracking system compensated for eye movements during data acquisition. To minimize the sensitivity roll-off (loss of sensitivity with increasing depth), the instrument was aligned to keep the B-scans during data acquisition as flat as possible and close to the position at which the optical path difference was zero (upper part of the live image). Raw data, including B-scan images and segmentation results for the RNFL, were exported.

Choroidal Thickness

Choroidal thickness was measured in two steps using software developed in high-level computing software (MatLab; MathWorks, Inc., Natick, MA) by one of the authors (MM). Raw data of the B-scans were imported to the software. In a first step, the RPE was automatically segmented and B-scans were flattened according to the RPE. Incorrect RPE segmentation could be corrected manually. In the second step, the choroidal-scleral interface could be segmented manually. The choroidal-scleral interface is the line between visible areas of vessels and the more homogeneous layer underneath. The developed software allows changing the contrast of the B-scans to optimize the visibility of this border for manual segmentation. For each B-scan, the distance between RPE and the choroidal-scleral interface results in 768 values for the peripapillary choroidal thickness. These 768 values were averaged to 32 sectors (11.25° each) and the total peripapillary mean. B-scans were not corrected for oblique incidence. The only subjects included in this study were those in whom the choroidal-scleral interface was completely visible in the B-scans. Twelve subjects of the initially selected subjects could not be included because the choroidal-scleral interface was not completely visible in their B-scans.

Statistical Analysis

The statistical significance of the demographic and clinical differences between the very typical group (TSS 100) and each other subgroup was evaluated using independent-samples tests with respect to continuous variables (TSS, age, refraction, visual field mean deviation, Nerve Fiber Index (NFI), RNFL thickness as determined by GDxVCC and Spectralis OCT, and choroidal layer thickness as determined by Spectralis-OCT). For differences in dichotomous variables between groups, we used the Pearson χ^2 test. Associations of TSS and choroidal layer thickness, age, spherical and cylindrical refractive error, NFI, age, and

TABLE 1. Demographic Characteristics and Results for NFI, RNFL Thickness (GDx VCC, and SDOCT), and Mean Choroidal Thickness in Four TSS Groups

	Very Typical	Typical	P*	Less Typical	P*	Atypical	P*
Subjects, n	36	37		20		17	
TSS	100 ± 0 (100-100)	95.4 ± 2.9 (90-99)	<0.001	85.1 ± 2.7 (81-89)	<0.001	59.8 ± 16.2 (32-79)	<0.001
Sex, n	14	13	0.740	5	0.293	5	0.502
Female	22	24		15		12	
Male							
Age, y	47.0 ± 13.8 (20-73)	51.2 ± 13.0 (23-77)	0.185	52.7 ± 13.6 (24-74)	0.148	54.9 ± 17.6 (22-73)	0.084
Spherical refraction, D	-0.13 ± 1.37 (-2.5-4.5)	-0.61 ± 1.7 (-4.25-3.25)	0.193	-0.74 ± 1.66 (-4.5-2.5)	0.149	-0.84 ± 1.79 (-4.25-1.5)	0.119
Cylindrical refraction, D	0.23 ± 0.38 (0-1.75)	0.39 ± 0.65 (0-3)	0.195	0.66 ± 1.1 (0-5.0)	0.116	0.38 ± 0.67 (0-2)	0.292
Visual field MD	-0.20 ± 1.39 (-2.4-3.2)	-0.01 ± 0.96 (-1.0-2.4)	0.500	-0.18 ± 1.1 (-2.1-2.1)	0.933	-0.21 ± 0.94 (-1.4-2.2)	0.987
NFI (GDx)	15.5 ± 8.3 (2-41)	13.5 ± 7.1 (2-24)	0.281	14.5 ± 6.8 (3-27)	0.631	14.1 ± 6.4 (2-28)	0.530
RNFL thickness (GDx), μm	54.2 ± 5.5 (41.7-65.3)	56.7 ± 4.3 (50.8-66.7)	0.038	57.8 ± 5.1 (49.1-66.3)	0.019	61.8 ± 5.1 (54.5-75.0)	<0.001
RNFL thickness (OCT), μm	94.5 ± 8.5 (80.0-116.0)	95.9 ± 7.1 (83.0-108.0)	0.482	95.7 ± 8.5 (81.0-115.0)	0.619	95.3 ± 12.0 (74.0-117.0)	0.483
Choroidal layer thickness (OCT), μm	168.5 ± 38.3 (117.0-250.7)	147.8 ± 47.9 (83.4-306.8)	0.046	119.1 ± 35.3 (62.7-213.7)	<0.001	91.9 ± 42.5 (43.9-208.1)	<0.001

Values are mean ± SD (range). TSS groups were statistically compared with the TSS 100 group. Differences between groups were tested for statistical significance with independent samples *t*-tests for continuous variables and with the Pearson χ^2 test for dichotomous variables. Bold type indicates results with statistically significant differences between groups.

RNFL thickness as determined by OCT and GDxVCC were evaluated using Spearman's correlation coefficient. $P < 0.05$ was considered statistically significant. Statistical analyses were performed using statistical software (SPSS, version 19.0; SPSS, Chicago, IL).

RESULTS

One hundred ten healthy subjects were included in this study. Table 1 compares demographic characteristics, refraction, visual field mean deviation (MD), NFI (GDx), RNFL thickness GDx, and RNFL thickness SDOCT and choroidal thickness among the four TSS groups. The distributions of the TSS values of all 110 healthy subjects are shown in Figure 1. The numbers of subjects in the different TSS groups were 36 subjects (33%) in the very typical group, 37 (34%) in the typical group, 20 (18%) in the less typical group, and 17 (15%) in the atypical group with TSS <80.

TSS correlated statistically significantly with choroidal layer thickness ($r = 0.608$; $P < 0.001$). TSS was inversely correlated with age ($r = -0.264$; $P = 0.005$) and RNFL thickness as determined by GDxVCC ($r = -0.389$; $P < 0.001$). There was no correlation of TSS with spherical and cylindrical refractive error, NFI, and RNFL mean thickness measured by SDOCT (Table 1).

Mean choroidal thickness (\pm SD) of all subjects was 141 μ m (\pm 49 μ m) and decreased considerably (mean \pm SD) from the TSS 100 group (168 μ m \pm 38) to the atypical group (92 μ m \pm 43 μ m) (see Table 1). Mean choroidal thickness in TSS groups 3 and 4 was significantly lower than in TSS group 1 ($P < 0.001$).

The distribution of choroidal thickness around the ONH was not uniform; instead, there was a significant reduction in thickness at approximately 270°, corresponding to the inferior position (Fig. 2). B-scan images of two subjects from different TSS groups are shown in Figure 3. The different choroidal thickness can be clearly seen in these images.

The distribution of choroidal thickness around the ONH in the four TSS groups is shown in Figure 4A. There was an almost uniform reduction in choroidal thickness around the ONH in the different TSS groups with decreasing TSS compared with the TSS 100 group, as shown in Figure 4B.

DISCUSSION

The appearance of ARP and decreasing TSS shows a high correlation with decreasing peripapillary choroidal thickness. Reduced choroidal thickness may result in an increased amount of light reflected from the strongly birefringent

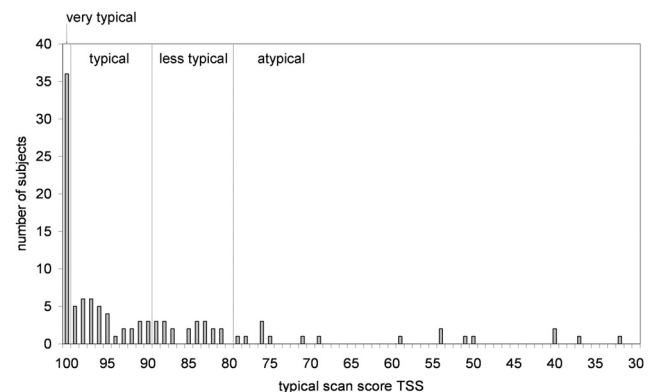


FIGURE 1. TSS distributions of 110 healthy subjects and the selected ranges for the four TSS groups: very typical (TSS 100), typical (TSS 90-99), less typical (TSS 80-89) and atypical (TSS <80).

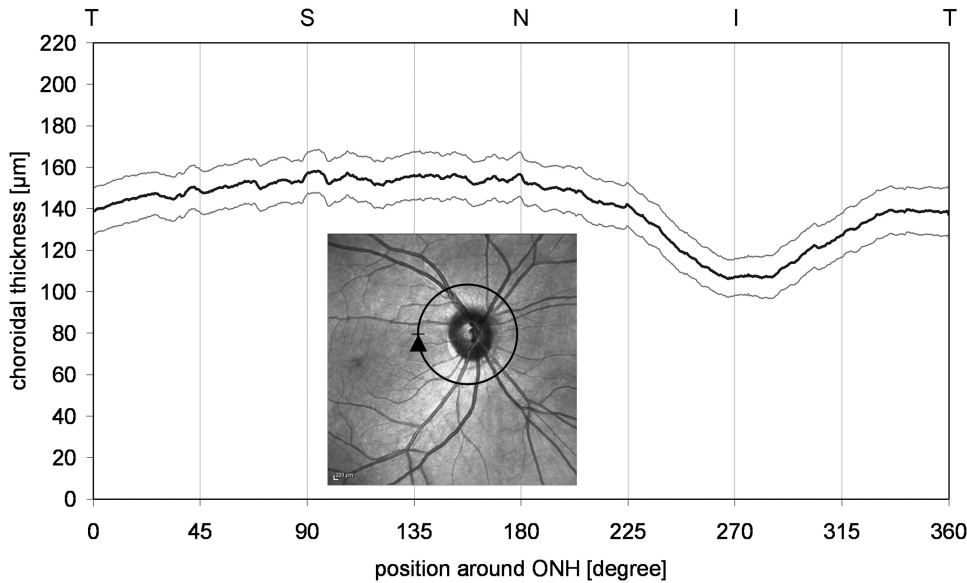


FIGURE 2. Mean peripapillary choroidal thickness (\pm 95% CI) of 110 healthy subjects. *Inset:* position and scan direction of the OCT B-scans for a right eye. In the right eye, 0° starts at 9 o'clock in the clockwise direction. In the left eye, 0° starts at 3 o'clock in the counterclockwise direction. T, temporal; S, superior; N, nasal; I, inferior.

sclera¹⁸ to the SLP light detectors. This signal contributes to the retardation of the probing light and interferes with the signal from the RNFL when choroidal thickness is low.

The amount of the confounding signal from the sclera depends on the optical properties (including changes of the polarization state of the light) of the different layers of the ocular fundus. The sclera is often considered the most important reflector in the fundus.^{19,20} However, the most important variable affecting the magnitude of the reflection of the fundus is the degree of melanin pigmentation of the fundus (RPE and choroidal stroma)¹⁹ and the light attenuation (absorption and scattering) by blood in the choroid. OCT results show that the inner segment/outer segment boundaries of the photoreceptors, the end tips of the photoreceptors, and the RPE are also

strong reflectors. Layers that change the polarization state of the probing light (besides the cornea and the RNFL) are the RPE/Bruch's membrane (BM) complex and the sclera. One layer of the RPE/BM complex maintains the polarization state of backscatter light, and the RPE scrambles the polarization state of backscattered light. It acts as a depolarizing layer, whereas the polarization state of the transmitted light is maintained.^{21,22} In contrast, the sclera shows birefringence, but little is known about the magnitude and axis orientation of this scleral birefringence.

For polarimetry in the eye, it is important that there are polarization-preserving reflectors. Huang and Knighton²³ show that the RNFL itself has the properties necessary to be the polarization-preserving reflector for SLP. They conclude that,

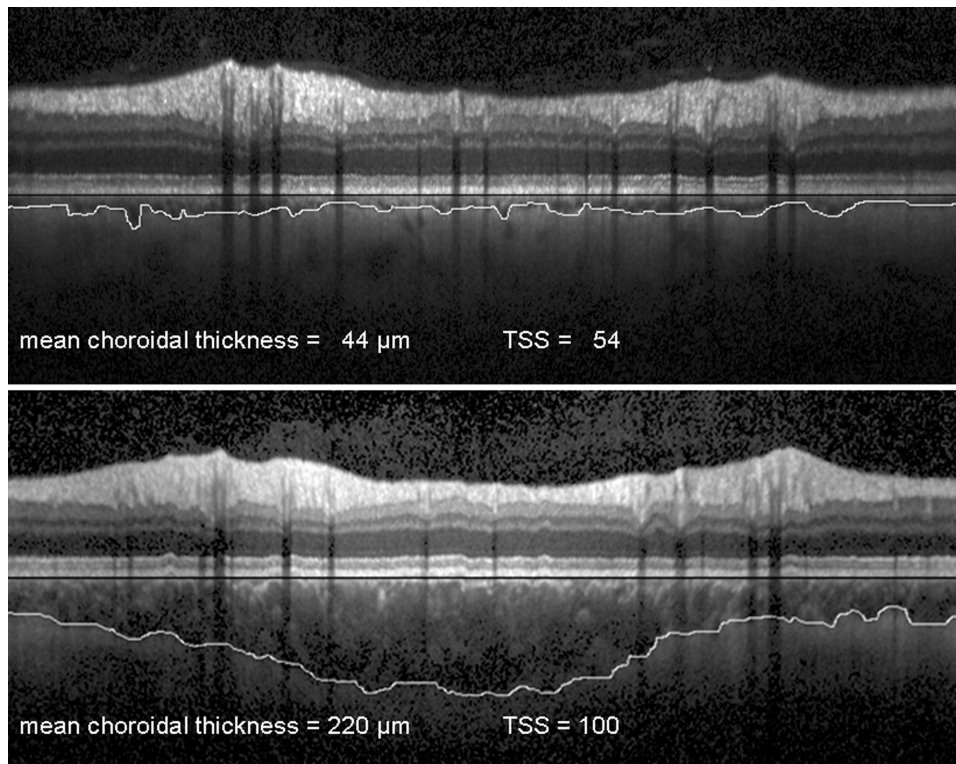


FIGURE 3. Examples of OCT B-scans showing two healthy subjects with different choroidal thickness. Mean choroidal thickness and TSS values are shown. B-scans are flattened so that the RPE results in a *straight line* (marked with a *black line*). The manually segmented choroidal-scleral interface is marked with a *gray line*.

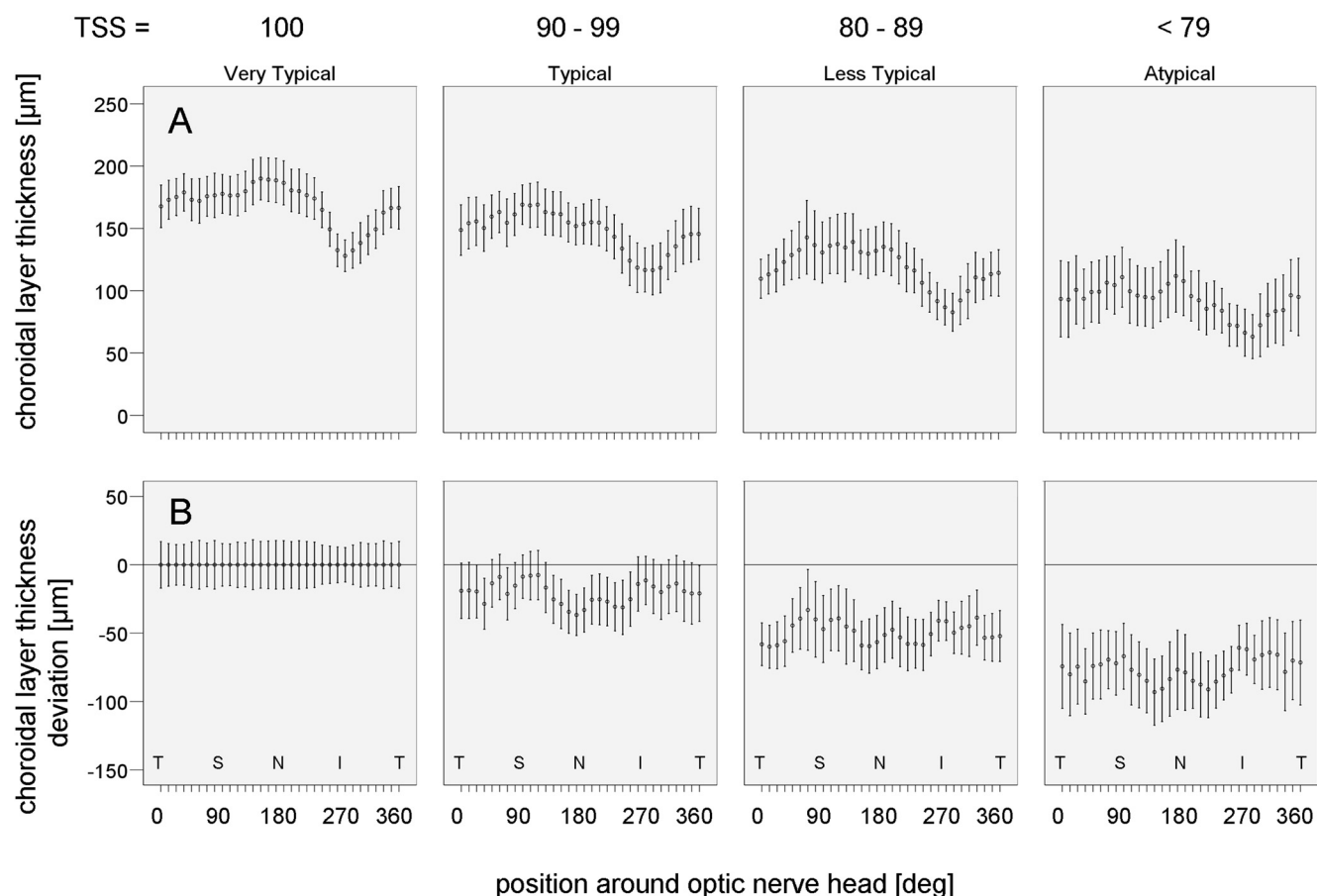


FIGURE 4. Peripapillary choroidal thickness in 32 sectors. (A) Mean peripapillary choroidal thickness ($\pm 95\%$ CI) in four TSS groups. (B) Deviation of the choroidal thickness in TSS groups from the thickness of TSS group 1. There is a nearly homogeneous reduction around the ONH with decreasing TSS.

as a consequence, the measured retardation of the RNFL in SLP could represent a single-pass value (light reflected only from within the RNFL), a double-pass value (light that passes the RNFL, is reflected at deeper layers, and passes the RNFL a second time), or some combination of the two.

Light that passes the RNFL and is reflected from the photoreceptor/BM/RPE complex is partly depolarized, but no additional retardation is introduced by this reflection, and this light does not contribute to the ARP. However, light that is reflected from the sclera may undergo additional retardation. If this light arrives at the detector, it has passed the choroid twice; hence, the amount of this light strongly depends on the attenuation in the choroid and also on its thickness.

Another way in which choroidal thickness could influence the appearance of ARP is the confocal configuration of the instrument. Different choroidal thicknesses lead to different distances between the plane of the source signal (RNFL) and the plane of the confounding signal (sclera) (compare the distances between the RNFL and the gray line [choroidal-scleral interface] in the two examples shown in Fig. 3). Assuming a mean distance between the lower boarder of the RNFL and the RPE (residual retinal thickness) of $220\ \mu\text{m}$ (Tornow RP, et al. *IOVS*. 2009;50:ARVO E-Abstract 1095), the average distance of the plane of the error source to the focal plane (distance = residual retinal thickness + choroidal thickness) increases by $77\ \mu\text{m}$ (25%) from $312\ \mu\text{m}$ (TSS <80) to $389\ \mu\text{m}$ (TSS = 100). This could explain, at least to a certain degree, the influence of the choroidal thickness on the appearance of ARP; however, this effect is probably only weak compared with the

light attenuation in the choroid. More research is necessary to clarify the underlying mechanism regarding reduced choroidal thickness and ARP; other parameters may also influence the appearance of ARP.

An interesting result from the anatomic point of view is that the inferior choroidal thickness was significantly thinner than were other areas. However, the reason for this reduced thickness is unknown. One explanation could be that, in the course of embryonal development, the ocular cleavage closes inferiorly. It is generally known that choroidal coloboma are most frequently found inferiorly if complete closing of the cleavage fails.²⁴ Another open question is whether this reduced thickness at the inferior position has an influence on the development of glaucoma. To date there is no evidence about whether the thinner choroidal thickness in the inferior region may correlate with early losses of nerve fibers in this region. Further studies that include glaucoma patients are necessary to answer these questions and are in progress.

In conclusion, it has been shown that ARP in SLP in healthy subjects is highly correlated with reduced peripapillary choroidal thickness. The high variability of choroidal thickness between healthy subjects can explain why some people show ARP in SLP and others do not. However, further studies must investigate the influence of other parameters, such as pigmentation of the choroid and the RPE and the polarization properties of the RPE/BM complex and the sclera on the appearance of ARP. This could help to improve SLP results in subjects with ARP.

References

- Swanson EA, Izatt JA, Hee MR, et al. In vivo retinal imaging by optical coherence tomography. *Opt Lett*. 1993;18:1864-1866.
- Ishikawa H, Piette S, Liebmann JM, Ritch R. Detecting the inner and outer borders of the retinal nerve fiber layer using optical coherence tomography. *Graefes Arch Clin Exp Ophthalmol*. 2002;240:362-371.
- Weinreb RN, Dreher AW, Coleman A, Quigley H, Shaw B, Reiter K. Histopathologic validation of Fourier-ellipsometry measurements of retinal nerve fiber layer thickness. *Arch Ophthalmol*. 1990;108:557-560.
- Bagga H, Greenfield DS, Feuer W, Knighton RW. Scanning laser polarimetry with variable corneal compensation and optical coherence tomography in normal and glaucomatous eyes. *Am J Ophthalmol*. 2003;135:521-529.
- Zhou Q. Retinal scanning laser polarimetry and methods to compensate for corneal birefringence. *Bull Soc Belge Ophthalmol*. 2006;89-106.
- Leung CK, Chan WM, Chong KK, et al. Comparative study of retinal nerve fiber layer measurement by StratusOCT and GDx-VCC, I: correlation analysis in glaucoma. *Invest Ophthalmol Vis Sci*. 2005;46:3214-3220.
- Schrems WA, Mardin CY, Horn FK, Juenemann AG, Laemmer R. Comparison of scanning laser polarimetry and optical coherence tomography in quantitative retinal nerve fiber assessment. *J Glaucoma*. 2010;19:83-94.
- Bagga H, Greenfield DS, Feuer WJ. Quantitative assessment of atypical birefringence images using scanning laser polarimetry with variable corneal compensation. *Am J Ophthalmol*. 2005;139:437-446.
- Schrems WA, Laemmer R, Hoesl LM, et al. Influence of atypical retardation pattern on the peripapillary retinal nerve fibre distribution assessed by scanning laser polarimetry and optical coherence tomography. *Br J Ophthalmol*. 2011: DOI bjo.2010.190074 [pii] 10.1136/bjo.2010.190074.
- Da Pozzo S, Marchesan R, Canziani T, Vattovani O, Ravalico G. Atypical pattern of retardation on GDx-VCC and its effect on retinal nerve fibre layer evaluation in glaucomatous eyes. *Eye*. 2006;20:769-775.
- Bowd C, Medeiros FA, Weinreb RN, Zangwill LM. The effect of atypical birefringence patterns on glaucoma detection using scanning laser polarimetry with variable corneal compensation. *Invest Ophthalmol Vis Sci*. 2007;48:223-227.
- Reus NJ, Zhou Q, Lemij HG. Enhanced imaging algorithm for scanning laser polarimetry with variable corneal compensation. *Invest Ophthalmol Vis Sci*. 2006;47:3870-3877.
- Medeiros FA, Bowd C, Zangwill LM, Patel C, Weinreb RN. Detection of glaucoma using scanning laser polarimetry with enhanced corneal compensation. *Invest Ophthalmol Vis Sci*. 2007;48:3146-3153.
- Mai TA, Reus NJ, Lemij HG. Diagnostic accuracy of scanning laser polarimetry with enhanced versus variable corneal compensation. *Ophthalmology*. 2007;114:1988-1993.
- Qiu K, Leung CK, Weinreb RN, et al. Predictors of atypical birefringence pattern in scanning laser polarimetry. *Br J Ophthalmol*. 2009;93:1191-1194.
- Medeiros FA, Alencar LM, Zangwill LM, Sample PA, Susanna R Jr, Weinreb RN. Impact of atypical retardation patterns on detection of glaucoma progression using the GDx with variable corneal compensation. *Am J Ophthalmol*. 2009;148:155-163 e151.
- Benítez-del-Castillo J, Martínez A, Regi T. Correlation between scanning laser polarimetry with and without enhanced corneal compensation and high-definition optical coherence tomography in normal and glaucomatous eyes. *Int J Clin Pract*. 2011;65(7):807-816.
- Gotzinger E, Pircher M, Baumann B, Hirn C, Vass C, Hitzenberger CK. Analysis of the origin of atypical scanning laser polarimetry patterns by polarization-sensitive optical coherence tomography. *Invest Ophthalmol Vis Sci*. 2008;49:5366-5372.
- Delori FC, Pflibsen KP. Spectral reflectance of the human ocular fundus. *Appl Opt*. 1989;28:1061-1077.
- van de Kraats J, Berendschot TT, van Norren D. The pathways of light measured in fundus reflectometry. *Vision Res*. 1996;36:2229-2247.
- Pircher M, Gotzinger E, Leitgeb R, Sattmann H, Findl O, Hitzenberger C. Imaging of polarization properties of human retina in vivo with phase resolved transversal PS-OCT. *Opt Express*. 2004;12:5940-5951.
- Michels S, Pircher M, Geitzenauer W, et al. Value of polarisation-sensitive optical coherence tomography in diseases affecting the retinal pigment epithelium. *Br J Ophthalmol*. 2008;92:204-209.
- Huang XR, Knighton RW. Theoretical model of the polarization properties of the retinal nerve fiber layer in reflection. *Appl Opt*. 2003;42:5726-5736.
- Naumann G. *Spezielle pathologische Anatomie Band 12*. Heidelberg: Springer Verlag; 1980.